INSTITUTE OF PHYSICS PUBLISHING PLASMA PHYSICS AND CONTROLLED FUSION

Plasma Phys. Control. Fusion **48** (2006) 169–183 doi:10.1088/0741-3335/48/2/001

Modelling of the penetration process of externally applied helical magnetic perturbation of the DED on the TEXTOR tokamak

Y Kikuchi[1], K H Finken[1], M Jakubowski[1], M Lehnen[1], D Reiser[1], G Sewell[2], R C Wolf[1] and the TEXTOR-team

[1] Institut fuer Plasmaphysik, Forschungszentrum Juelich GmbH, EURATOM Association, D-52425, Germany
[2] Mathematics Department, Texas A&M University, College Station, TX, USA

Received 26 July 2005, in final form 13 October 2005
Published 4 January 2006
Online at stacks.iop.org/PPCF/48/169

Abstract

The error-field penetration process of the dynamic ergodic divertor (DED) on the TEXTOR tokamak has been investigated analytically in terms of a single fluid MHD model with a finite plasma resistivity and viscosity in a cylindrical geometry. The linear model produces a localization of the induced current at the resonance surface and predicts a vortex structure of the velocity field near the resonance layer. Moreover, effects of the Alfvén resonance for the error-field penetration are identified by two peaks in the radial profiles of the perturbed toroidal current and the perturbed magnetic flux when the relative rotation velocity between the DED and the rotating tokamak plasma is set to large. Fine structures of the vorticity induced by the DED in the vicinity of the rational surface disappear by introducing a finite plasma perpendicular viscosity. In addition, it is shown that the two peaks of the perturbed toroidal current overlap by an anomalous plasma perpendicular viscosity. Likewise, a bifurcation of the penetration process from the suppressed to the excited state is obtained by a quasi-linear approach taking into account modifications of the radial profiles of the equilibrium current and the plasma rotation due to the DED. A comparison with real experimental results of the DED on the TEXTOR tokamak is shown.

(Some figures in this article are in colour only in the electronic version)

1. Introduction

Two different types of magnetic field line reconnections are treated in tokamak plasmas [1]: one is driven spontaneously due to internal MHD instabilities such as tearing modes or changes of plasma equilibrium. Tearing mode is unstable if the well-known stability index Δ' is positive, which was first introduced by Furth *et al* [2]. From the stability analysis of the tearing mode, one can find that the tearing mode with a low m/n mode number tends to be unstable, where m

is the poloidal mode number and n is the toroidal mode number. The second one is a so-called forced magnetic reconnection, which can be caused by externally applied resonant magnetic perturbations on an equilibrium for which Δ' is negative [3–6].

Error-fields are well known as one of the externally applied resonant magnetic perturbations. Error-fields inevitably occur in real tokamak devices in terms of small deviations of tokamak magnetic fields from ideal axisymmetry, resulting from misalignments of magnetic field coils, nonaxisymmetric coil feeders and connections. Magnetic islands driven by error-fields with low m/n mode numbers give rise to a significant degradation of energy confinement or major disruptions. Simulation experiments of error-fields in several tokamak devices, which are equipped with coils external to the tokamak plasmas, have been carried out in order to clarify error-field sensitivity on next step tokamak devices such as ITER [7–9]. These experimental results indicate that when the amplitude of the error-fields exceeds a critical value, the plasma rotation velocity drops suddenly, and large magnetic islands are generated. The mechanism of this nonlinear behaviour, a so-called 'mode penetration' has also been investigated theoretically, in which a suppression of the error-field driven magnetic island formation due to a plasma rotation is addressed [10–12].

The dynamic ergodic divertor (DED) [13] experiment has been started on the TEXTOR tokamak in order to investigate comprehensive understandings of the plasma responses to the externally imposed static (dc) and rotating (ac) magnetic perturbations. The description of the DED and the TEXTOR will be shown in detail in the next section. Experimental results with the DED of $m/n = 3/1$ basic mode show that $m/n = 2/1$ tearing type mode was triggered due to the strong sideband component of the magnetic perturbation of $m/n = 2/1$ when the DED coil current was above the critical threshold [14–17]. The dynamic operation of the DED in combination with a control of the toroidal plasma rotation by two tangential neutral beam injections (NBIs) has an advantage to understand effects of the relative rotation between the tokamak plasma and the magnetic perturbations on the threshold of the required DED coil current for the mode penetration.

In this paper, we investigate the dynamic behaviour of the penetration process of the DED field into rotating tokamak plasma by solving a reduced set of resistive and viscous MHD equations in a cylindrical geometry. The MHD equations are linearized, and an equilibrium poloidal magnetic field and a plasma rotation are prescribed which is iterated by a quasi-linear approach. From the linear calculations, error-field amplifications (suppressions) by the plasma in the cases of not only static perturbations but also dynamic ones will be shown. Moreover, effects of the Alfvén resonances on the penetration process of the DED will be discussed. Likewise, a quasi-linear calculation has been carried out in order to clarify the dynamics of the interactions between the DED and the rotating tokamak plasmas.

The paper is organized as follows: after a description of the DED, basic equations with boundary and initial conditions are presented in section 2. Numerical results of the linear and quasi-linear calculations are shown in section 3. Some real experimental results of the DED on the TEXTOR are discussed in comparison with the numerical results in section 4. Finally, we summarize our results in section 5.

2. Description of the DED and model equations

2.1. Description of the DED

In the TEXTOR tokamak (major radius $R_0 = 1.75$ m, minor radius of circular plasma cross section typically $a = 0.47$ m) the DED coils have been installed inside the vacuum vessel at the high field side of the torus as shown in figure 1(*a*). The coils wind with a helical

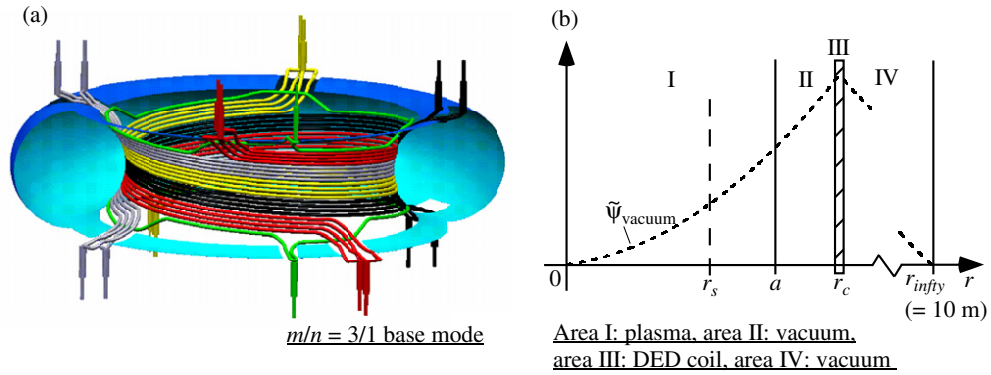

Figure 1. (*a*) Schematic view of the DED coils on the TEXTOR tokamak. Here, the configuration of the $m/n = 3/1$ basic mode is presented. (*b*) Analytical model of the present work: area I represents the tokamak plasma, areas II and IV are vacuum and area III represents the DED coil.

pitch corresponding to the equilibrium magnetic field lines of the flux surface with a safety factor of $q = 3$. The unique feature of the DED is the capability to apply rotating magnetic perturbation fields with a frequency of up to 10 kHz. Depending on the coil connections, basic mode numbers of the DED are $m/n = 12/4$, $6/2$ or $3/1$. While the $m/n = 12/4$ mode decays radially rather quickly, affecting mainly the plasma edge, the perturbation field of the $m/n = 3/1$ configuration penetrates deeply into the plasma. Accordingly, the main application of the first is the study of the divertor properties with the edge ergodization [18, 19], while the latter is mainly used to study excitation of error-field modes. The intermediate $m/n = 6/2$ configuration has not been used up to now.

Different poloidal mode numbers of the DED field can be generated either by effects of toroidicity or the coil structures. Since the DED covers less than 1/3 of the poloidal circumference, the mode spectra contain always strong sideband components. Mode analyses of the magnetic perturbations of the DED in vacuum, in which the real coil configuration and the toroidal effects are taken into account, have been carried out [20]. The mode spectra of the DED show that a strong sideband component of $m/n = 2/1$ is generated when the $m/n = 3/1$ configuration of the DED is set. Real experimental results with the DED configuration of $m/n = 3/1$ in the TEXTOR tokamak indicate that an error-field mode of $m/n = 2/1$ was mainly excited at $q = 2$, but the mode of $m/n = 3/1$ was not identified [14–17]. Therefore, the strong sideband component of $m/n = 2/1$ is addressed in this paper.

2.2. Model equations

A linearized set of single fluid MHD equations with the plasma resistivity and the plasma viscosity as the dissipative terms is adopted.

$$\rho\left\{\frac{\partial\tilde{\boldsymbol{v}}}{\partial t} + (\boldsymbol{v}_0\cdot\nabla)\,\tilde{\boldsymbol{v}} + (\tilde{\boldsymbol{v}}\cdot\nabla)\boldsymbol{v}_0\right\} = -\nabla\tilde{p} + \tilde{\boldsymbol{j}}\times\boldsymbol{B}_0 + \boldsymbol{j}_0\times\tilde{\boldsymbol{B}} + \mu_\perp\nabla^2\tilde{\boldsymbol{v}}, \quad (1)$$

$$\tilde{\boldsymbol{E}} + \tilde{\boldsymbol{v}}\times\boldsymbol{B}_0 + \boldsymbol{v}_0\times\tilde{\boldsymbol{B}} = \eta\tilde{\boldsymbol{j}}, \quad (2)$$

$$\nabla\times\tilde{\boldsymbol{E}} = -\frac{\partial\tilde{\boldsymbol{B}}}{\partial t}, \quad (3)$$

$$\nabla\times\tilde{\boldsymbol{B}} = \mu_0\tilde{\boldsymbol{j}}, \quad (4)$$

where the superscript $\sim$, the subscripts 0, ρ, μ_0, $\mu_\perp$, η denote the perturbed fields, the equilibrium fields, the plasma mass density, the permeability of free space, the plasma perpendicular viscosity and the plasma resistivity, respectively. Standard right-hand cylindrical polar co-ordinates (r, θ, z) are adopted. The plasma is assumed to be periodic in the z-direction with periodicity length $2\pi R_0$, where R_0 is the simulated major radius. The equilibrium magnetic fields and velocities are written as

$$\boldsymbol{B}_0 = (0, B_{\theta 0}(r), B_{z0}), \qquad \boldsymbol{v}_0 = (0, v_{\theta 0}(r), v_{z0}(r)). \tag{5}$$

The safety factor is defined by

$$q(r) = \frac{r B_{z0}}{R_0 B_{\theta 0}} \tag{6}$$

and the equilibrium toroidal current is given by

$$j_{z0}(r) \simeq \frac{1}{\mu_0 r}\frac{\partial}{\partial r}(r B_{\theta 0}) = \frac{B_{z0}}{R_0 \mu_0}\frac{1}{r}\frac{\partial}{\partial r}\Big(\frac{r^2}{q}\Big). \tag{7}$$

By introducing a perturbed magnetic flux $\tilde{\psi}$ and a perturbed stream function $\tilde{\phi}$, the perturbed magnetic fields and velocities are described as

$$\tilde{\boldsymbol{B}} = \nabla\tilde{\psi} \times \boldsymbol{e}_z = \Big(\frac{\mathrm{i}m}{r}\tilde{\psi}, -\frac{\partial\tilde{\psi}}{\partial r}, 0\Big), \qquad \tilde{\boldsymbol{v}} = \nabla\tilde{\phi} \times \boldsymbol{e}_z = \Big(\frac{\mathrm{i}m}{r}\tilde{\phi}, -\frac{\partial\tilde{\phi}}{\partial r}, 0\Big), \tag{8}$$

where an $\exp[\mathrm{i}(m\theta - nz/R_0)]$ dependence of the perturbed quantities is assumed.

The differential equations for the perturbed quantities can be written as follows:

$$\frac{\partial\tilde{U}}{\partial t} = \frac{\mathrm{i}m}{\rho\mu_0 r}\Big\{B_{\theta 0}(1 - nq/m)\Delta_\perp\tilde{\psi} - \mu_0\frac{\partial j_{z0}}{\partial r}\tilde{\psi}\Big\} + \frac{\mu_\perp}{\rho}\Delta_\perp\tilde{U}$$
$$-\Big(\frac{\mathrm{i}m}{r}v_{\theta 0} - \frac{\mathrm{i}n}{R_0}v_{z0}\Big)\tilde{U} + \frac{\mathrm{i}n}{R_0}\frac{\partial v_{z0}}{\partial r}\frac{\partial\tilde{\phi}}{\partial r} + \frac{\mathrm{i}m}{r}\Big(\frac{\partial^2 v_{\theta 0}}{\partial r^2} + \frac{1}{r}\frac{\partial v_{\theta 0}}{\partial r} - \frac{1}{r^2}v_{\theta 0}\Big)\tilde{\phi}, \tag{9}$$

$$\frac{\partial\tilde{\psi}}{\partial t} = \frac{\eta}{\mu_0}\Delta_\perp\tilde{\psi} + \frac{\mathrm{i}m}{r}B_{\theta 0}(1 - nq/m)\tilde{\phi} - \Big(\frac{\mathrm{i}m}{r}v_{\theta 0} - \frac{\mathrm{i}n}{R_0}v_{z0}\Big)\tilde{\psi}, \tag{10}$$

$$\tilde{U} = \Delta_\perp\tilde{\phi}, \qquad \Delta_\perp = \frac{1}{r}\frac{\partial}{\partial r}\Big(r\frac{\partial}{\partial r}\Big) - \frac{m^2}{r^2}, \tag{11}$$

where $\tilde{U}$ is the perturbed vorticity. It is noticed that the branch of the compressional Alfvén wave is eliminated in the above equations [21].

Nonlinearities are included in terms of the following quasi-linear approach [22, 23].

$$\frac{\partial B_{\theta 0}}{\partial t} = \frac{1}{\mu_0}\frac{\partial}{\partial r}\Big(\frac{\eta}{r}\frac{\partial}{\partial r}(r(B_{\theta 0} - B_{\theta 0}|_{t=0}))\Big)$$
$$+\frac{1}{2}\Im_m\Big[\frac{m}{r^2}\Big(\tilde{\psi}^*\frac{\partial\tilde{\phi}}{\partial r} + \tilde{\phi}\frac{\partial\tilde{\psi}^*}{\partial r}\Big) - \frac{m}{r}\Big(\tilde{\psi}^*\frac{\partial^2\tilde{\phi}}{\partial r^2} + \tilde{\phi}\frac{\partial^2\tilde{\psi}^*}{\partial r^2} + 2\frac{\partial\tilde{\phi}}{\partial r}\frac{\partial\tilde{\psi}^*}{\partial r}\Big)\Big], \tag{12}$$

$$\rho\frac{\partial v_{\theta 0}}{\partial t} = \frac{1}{r^2}\frac{\partial}{\partial r}\Big(\mu_\perp r^3\frac{\partial}{\partial r}\Big(\frac{1}{r}(v_{\theta 0} - v_{\theta 0}|_{t=0})\Big)\Big) - \rho\mu_\parallel(v_{\theta 0} - v_{\theta 0}|_{t=0})$$
$$-\frac{m}{2\mu_0 r}\Im_m(\tilde{\psi}^*\Delta_\perp\tilde{\psi}) - \frac{\rho m}{2r}\Im_m\Big(\tilde{\phi}\frac{\partial^2\tilde{\phi}^*}{\partial r^2} - \frac{1}{r}\tilde{\phi}^*\frac{\partial\tilde{\phi}}{\partial r}\Big), \tag{13}$$

$$\rho\frac{\partial v_{z0}}{\partial t} = \frac{1}{r}\frac{\partial}{\partial r}\Big(\mu_\perp r\frac{\partial}{\partial r}(v_{z0} - v_{z0}|_{t=0})\Big)$$
$$+\frac{n}{2\mu_0 R_0}\Im_m(\tilde{\psi}^*\Delta_\perp\tilde{\psi}) + \frac{\rho n}{2R_0}\Im_m\Big(\tilde{\phi}\frac{\partial^2\tilde{\phi}^*}{\partial r^2} - \frac{1}{r}\tilde{\phi}^*\frac{\partial\tilde{\phi}}{\partial r}\Big), \tag{14}$$

where $\mu_\parallel$, superscript $*$ and $\Im_m$ are the neoclassical parallel viscosity in the poloidal direction ($\sim 7 \times 10^5\ \mathrm{s}^{-1}$), the conjugate complex and the imaginary part of the complex value, respectively. It is assumed that the initial states of the radial profiles of the equilibrium current density and the plasma rotation are kept unless the DED is applied. The $\mu_\perp$ and the $\mu_\parallel$ are assumed to be constant in the radial direction.

The computational domain includes vacuum regions between the plasma and the DED coil and outside the DED coil as shown in figure 1(*b*). The perturbations are assumed to be continuous at the transition of the different areas. At the axis ($r = 0$) and at infinity ($r = 10\,\mathrm{m}$) the perturbations are set to zero. The $\tilde{\phi}$ is set to be zero outside the plasma region ($r > a$, a: plasma radius). The DED coil current is assumed to be a form of $\exp \mathrm{i}(m\theta - nz/R_0 - \omega_{\mathrm{DED}}t)$, where ω_{DED} is the angular frequency of the DED. Here, the Doppler-shifted angular frequency of the DED with respect to the rotating tokamak plasma is written as $\omega' = \omega_{\mathrm{DED}} - \{(m/r)v_{\theta 0} - (n/R_0)v_{z0}\}$. The initial values of all the perturbations are set to zero. The initial profile of the equilibrium current density is taken as $j_{z0} = (\nu + 1)I_{\mathrm{p}}(1 - (r/a)^2)^\nu/\pi a^2$. Here, I_{p} and ν are the plasma current and the peaking factor of j_{z0}, respectively.

For the numerical treatment, the present time-dependent and one-dimensional problem of the differential equations was solved by the PDE2D code (finite element solver) [24] with the above boundary and initial conditions. Radial meshes in the code are dense near the resonance surface and the DED coil to ensure the spatial resolution. The time step is set to 1×10^{-8} s (the Alfvén transit time τ_A is typically 6×10^{-8} s). The PDE2D code uses implicit methods, so that the numerical stability is not restricted by a well-known Courant–Freidrichs–Lewy condition.

3. Numerical results

3.1. Linear calculations

3.1.1. Static magnetic perturbation. The strong $m/n = 2/1$ sideband component which is created by the DED configuration of the $m/n = 3/1$ is considered in this paper. The peaking factor ν of the equilibrium current is chosen as the original equilibrium is stable for current driven tearing modes. The tearing mode stability parameter Δ'_0 is calculated by the following equation which is derived from equation (9) by neglecting the plasma inertia, the plasma viscosity and the equilibrium plasma flow.

$$\frac{\partial^2\tilde{\psi}}{\partial r^2} + \frac{1}{r}\frac{\partial\tilde{\psi}}{\partial r} - \left(\frac{m^2}{r^2} + \frac{\mu_0 \partial j_{z0}/\partial r}{B_{\theta 0}(1 - nq/m)}\right)\tilde{\psi} = 0, \tag{15}$$

$$\Delta'_0 = (\tilde{\psi}'(r_{\mathrm{s}} + \epsilon) - \tilde{\psi}'(r_{\mathrm{s}} - \epsilon))/\tilde{\psi}(r_{\mathrm{s}}), \qquad \epsilon \to 0, \tag{16}$$

where r_{s} is the rational surface. The calculated Δ'_0 of $\nu = 8, 10$ and 12 are -3.0, -5.2 and -8.4, respectively. In the analyses the plasma current, the toroidal magnetic field, the electron temperature and density at $q = 2$ are set to 300 kA, 2.25 T, 500 eV and $2 \times 10^{19}\ \mathrm{m}^{-3}$, respectively. The skin depth $\delta(= \sqrt{\eta/(\mu_0\omega_{\mathrm{DED}})})$ of the DED field in the case of 1 kHz and the Lundquist number $S(= \tau_R/\tau_A$, τ_R: the current diffusion time, τ_A: the Alfvén wave transit time) are 3.2 mm and 6×10^7, respectively. The accuracy of the developed code was confirmed by comparing with the linear growth rate of tearing mode [1].

Figure 2 shows the time evolutions of the penetration of the DED, where the $f_{\mathrm{DED}} = \omega_{\mathrm{DED}}/2\pi$, the $\mu_\perp$ and the equilibrium plasma rotation velocities are set to zero. Here, the DED coil current is given as a step function at $t = 0$. It is shown that a negative perturbed current $\tilde{j}_z$ with the finite radial extent is induced around the rational surface just after applying

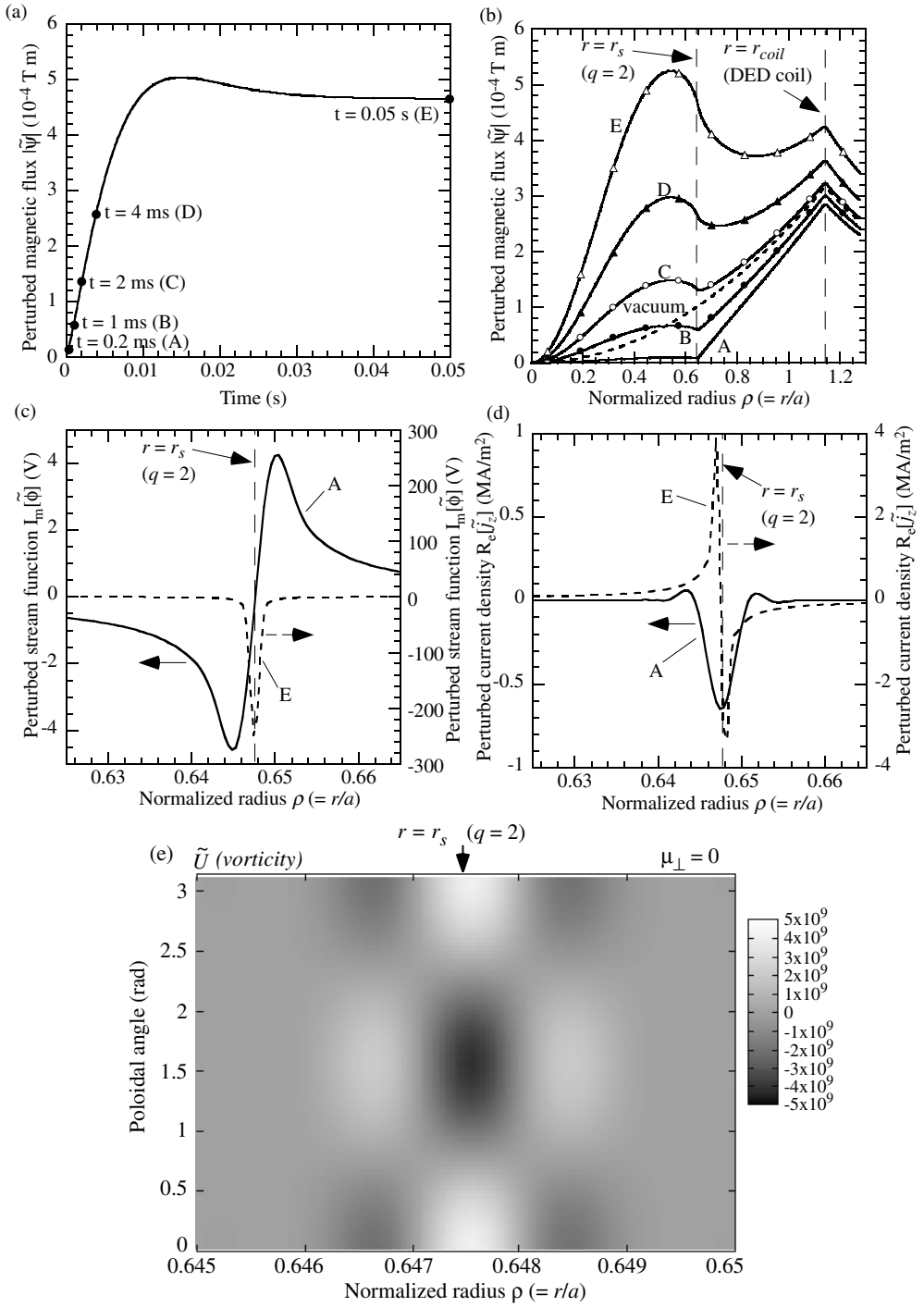

Figure 2. (*a*) Time evolutions of the calculated $\tilde{\psi}$ at the rational surface with $f_{\mathrm{DED}} = 0$, $\mu_\perp = 0$. (*b*) Radial profiles of $\tilde{\psi}$ at $t = 0.2$ ms (A), 1 ms (B), 2 ms (C), 4 ms (D), 0.05 s (E). The dashed line denotes that in vacuum. Radial profiles of (*c*) $\tilde{\phi}$ and (*d*) $\tilde{j}_z$ at $t = 0.2$ ms (A) and $t = 0.05$ s (E). (e) Contour of the vorticity $\tilde{U}$ at $t = 0.05$ s (E).

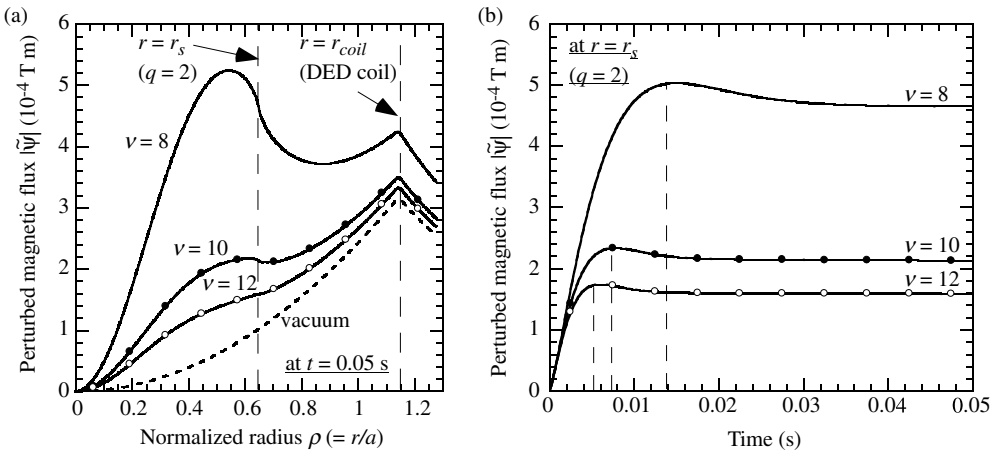

Figure 3. Dependence of the penetration on the initial current density profile. (*a*) Radial profiles of the $\tilde{\psi}$ at $t = 0.05$ s with $\nu = 8$, 10 and 12. (*b*) Time evolutions of the $\tilde{\psi}$ at the rational surface with $\nu = 8$, 10 and 12.

the DED ($t = 0.2$ ms (A) in figure 2(*d*)). The growth of the $\tilde{\psi}$ is determined by the sign of the $\tilde{j}_z$ at the rational surface, because the $\tilde{\psi}$ can be written as $\partial\tilde{\psi}/\partial t \sim -\eta\tilde{j}_z$. The spatial structure of the $\tilde{j}_z$ is changed in time, so that the transition from a suppressed to a fully reconnected state (error-field amplification) occurs as shown in figure 2(*b*). In figure 2(*e*) the calculated perturbed vorticity $\tilde{U}$ at the final stage ($t = 0.05$ s (E)) is shown, in which vortex patterns are produced by the DED in the vicinity of the rational surface. The amount of the error-field amplification and the time scale of the bifurcation of the magnetic reconnection depend on the initial equilibrium (i.e. Δ'_0) as shown in figure 3. These behaviours can also be seen in the theory of forced magnetic reconnection [3–6]. Here, it is noticed that the linear regime is valid only when the induced magnetic island width is smaller than that of the linear tearing layer [25].

3.1.2. Dynamic magnetic perturbation. Several investigations of the penetration process of the dynamic magnetic perturbation fields into a tokamak plasma in a quasi-steady state have been performed [27, 28]. Combining equations (9) and (10) in the present model, one finds the following dispersion relation of shear Alfvén wave.

$$\omega_{\mathrm{DED}}^2 = k_\parallel^2 v_A^2, \qquad k_\parallel = \frac{1}{R_0}\left(\frac{m}{q} - n\right), \tag{17}$$

where $k_\parallel$ and v_A represent the parallel wave number of the perturbation and the Alfvén velocity. Here, it is assumed that the perturbations have a time dependence of $\exp(-\mathrm{i}\omega_{\mathrm{DED}}t)$. Therefore, the present model includes two Alfvén resonance points at both sides of the rational surface ($k_\parallel = 0$). In [28] effects of the Alfvén resonance on the penetration process of the DED at the plasma edge ($q = 3$) have been discussed. It has been shown that effects of the dissipation of the plasma resistivity around the rational surface are dominant in comparison with those of the Alfvén resonance. On the other hand, the $m/n = 2/1$ sideband component of the DED, which interacts with a high temperature plasma at $q = 2$, is considered in this study. Therefore, the width of the resistive layer around the rational surface could be smaller than the radial distance between the two Alfvén resonance points.

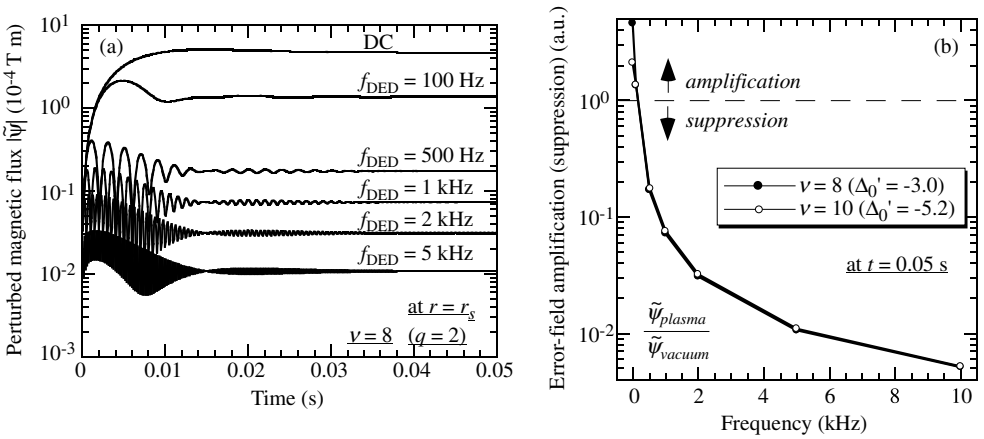

Figure 4. Dependence of the penetration on the DED frequency. (*a*) Time evolutions of the $\tilde{\psi}$ at the rational surface in the cases of the $f_{DED} = 0$, 100 Hz, 500 Hz, 1 kHz, 2 kHz and 5 kHz. (*b*) Amplitudes of the $\tilde{\psi}_{plasma}/\tilde{\psi}_{vacuum}$ at the rational surface.

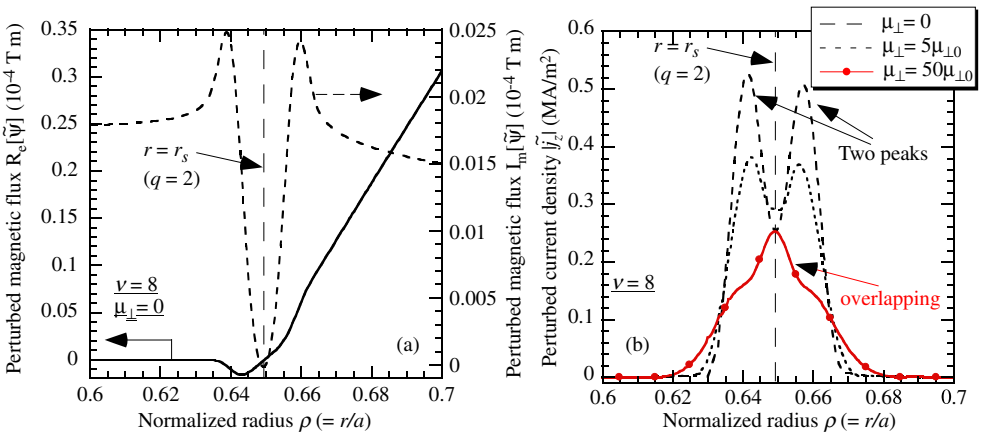

Figure 5. Radial profiles of (*a*) the $\tilde{\psi}$ and (*b*) the $\tilde{j}_z$ in the case of the high Doppler-shifted angular frequency, ω'. Here, the f_{DED}, the $v_{\theta 0}$ and the v_{z0} are set to 10 kHz, $-5\,\mathrm{km\,s^{-1}}$ and $40\,\mathrm{km\,s^{-1}}$, respectively.

Figure 4 shows the time evolutions of the $\tilde{\psi}$ in the case of dynamic magnetic perturbations. When increasing the DED frequency, the amount of the amplification of the $\tilde{\psi}$ at $q = 2$ is reduced by an eddy current flow near the resonance layer. It is shown that the amount of the magnetic reconnection, $\tilde{\psi}_{plasma}/\tilde{\psi}_{vacuum}$, at the rational surface is strongly suppressed in the case of the high DED frequency. On the other hand, the dependence of the suppression of the magnetic reconnection on the parameter ν is very weak in comparison with that of the amplification (figure 3(*a*)).

When the Doppler-shifted frequency of the DED is very high ($f' = \omega'/2\pi \sim 20$ kHz), the contributions of the Alfvén resonances on the penetration process of the DED into the tokamak plasma are not hindered in comparison with the dissipation due to the plasma resistivity as shown in figure 5. The two peaks in the radial profiles of the $\tilde{\psi}$ and the $\tilde{j}_z$ are identified at the locations of the Alfvén resonance points. In this case, the magnetic reconnection at the rational surface is strongly suppressed. A mode conversion to an electrostatic wave at the

Alfvén resonance points has been considered as one of the interactions between the DED and the tokamak plasma [29]. It has been shown that the resulting ponderomotive force could transfer from the DED to the tokamak plasma.

3.1.3. Effects of plasma viscosity. Effects of an anomalous plasma viscosity induced by the stochastization of magnetic field lines on tearing modes have been investigated in order to clarify fast sawtooth crashes in tokamaks [30, 31]. These results show that an anomalous plasma (ion) viscosity could suppress the growth of the tearing mode. In this study, effects of the plasma viscosity on the penetration process of the DED are investigated. As shown in [32] an anomalous perpendicular viscosity is necessary to explain the observations of the toroidal rotation in the TEXTOR. Therefore, the perpendicular viscosity $\mu_\perp$ is set to a large value compared with the neoclassical one $\mu_{\perp 0} (= 7.8 \times 10^{-10}\,\mathrm{kg\,m^{-1}\,s^{-1}})$.

Figure 6(*a*) shows the perturbed vorticity $\tilde{U}$ for the case without the plasma viscosity. Vortex structures are identified in the vicinity of the rational surface as well as the case of the static DED. The fine structures of the vorticity give rise to a strong shear flow around the rational surface. In addition to that, large structures of the vorticity are found at both sides of the rational surface. When a finite plasma viscosity is set, the fine structures of the vorticity in the vicinity of the rational surface are suppressed as shown in figure 6(*b*). It is noticed that the small value of the plasma viscosity ($\mu_\perp = 0.01\mu_{\perp 0}$) can smear out the shear flow around the rational surface. Even though there is no large difference between figures 6(*b*) and (*c*), an anomalous plasma viscosity ($\mu_\perp = 50\mu_{\perp 0}$) can broaden the large structures of the vorticity as shown in figure 6(*d*). In addition, the two peaks observed in the radial profile of the perturbed toroidal current $\tilde{j}_z$ overlap by the anomalous plasma viscosity as shown in figure 5(*b*). When the radial distance between the two Alfvén resonance points is large enough (e.g. high driving frequency of the external magnetic perturbation), the overlapping due to the plasma viscosity does not appear.

3.2. Quasi-linear calculations

Nonlinear interaction between the DED and the tokamak plasma is distinguished into two features. The first is usual nonlinearity, namely changes of background quantities of the current density profile and the plasma rotation profiles due to the error-fields. The second is an ergodization of the background magnetic field produced by an overlapping of the magnetic islands. The present study focuses on the first (resonant) feature, but the latter will be discussed in the final section by comparing with the experimental observations on the TEXTOR.

In order to clarify the nonlinear behaviour of the error-field penetration process, quasi-linear calculations have been performed, in which changes of the radial profiles of the equilibrium poloidal field (equation (12)) and the toroidal rotation velocity (equation (14)) due to the DED are taken into account. The present model with the quasi-linear approximation does not take into account effects of the higher harmonics and a deformation of the magnetic island due to the plasma flow. In the experiment of the DED, MHD modes with high frequencies were identified with Mirnov coils as one of the secondary effects of the mode penetration [33]. However, their effects are beyond the scope of the present work since we focus on the onset behaviour of the mode penetration.

The initial profile of the toroidal rotation v_{z0} is set so as to agree with the experimental observations on the TEXTOR [14, 17]. The contributions of the poloidal rotation to the Doppler-shifted frequency will be discussed in the next section. Thus, equation (13) is not taken into account in this section. It should be noted that the present model neglects the contribution of the gradient of the plasma pressure on the momentum balance equations. In

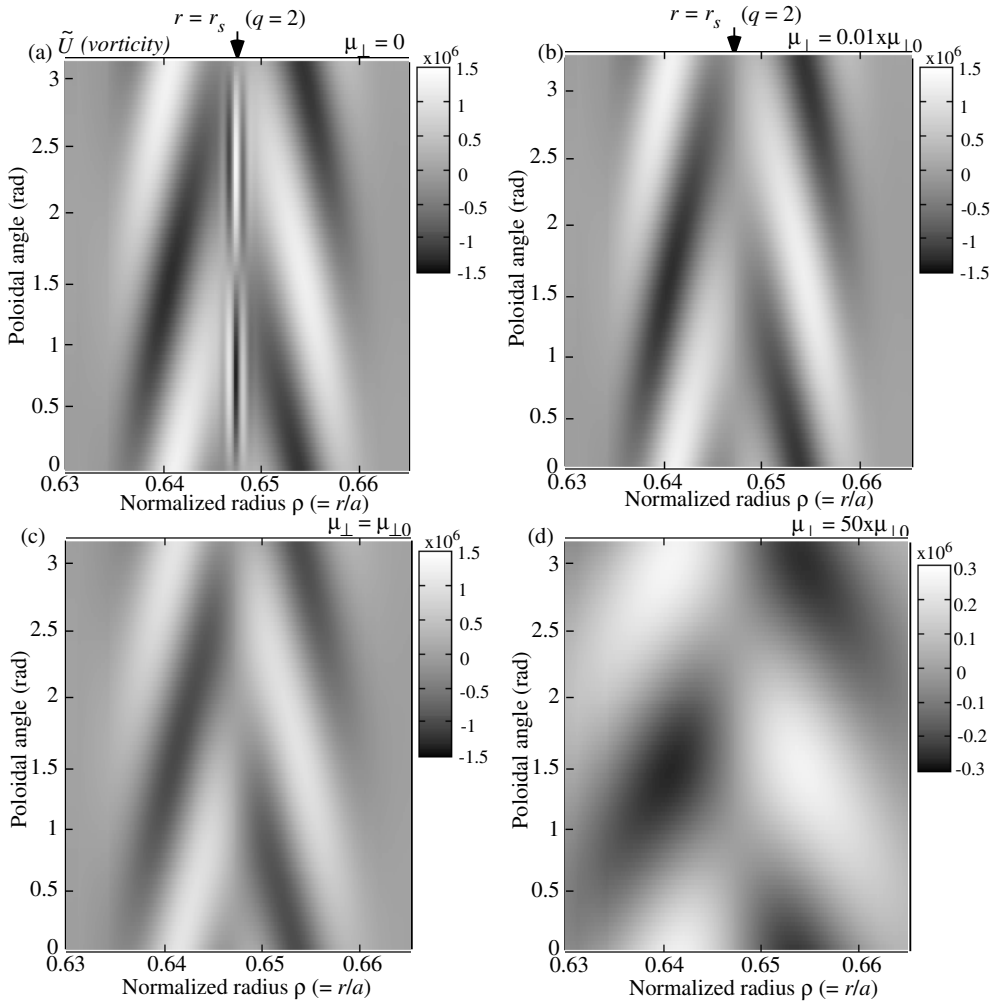

Figure 6. Contour plots of the vorticity $\tilde{U}$ for the cases with and without the plasma viscosity. (*a*) $\mu_\perp = 0$, (*b*) $\mu_\perp = 0.01\mu_{\perp 0}$, (*c*) $\mu_\perp = \mu_{\perp 0}$, (*d*) $\mu_\perp = 50\mu_{\perp 0}$. Here, the frequency of the DED is set to 10 kHz.

addition, when there is no external perturbation field, the equilibrium plasma rotation profiles will keep the initial states.

Figure 7(*a*) shows the typical result of the time evolutions of the toroidal rotation and the $\tilde{\psi}$ at the rational surface, where the DED coil current is ramped up linearly in time. The corresponding radial profiles of the v_{z0} are shown in figure 7(*b*). It is shown that the amount of the magnetic reconnection is strongly suppressed by the plasma rotation just after applying the DED. However, a slowing down of the v_{z0} is caused by the nonlinear $\tilde{j} \times \tilde{B}$ force induced by the DED. Figure 8 shows the total induced torque which is written as $F_{\text{total}} = F_{\tilde{j}\times\tilde{B}} + F_{\text{viscosity}} + F_{\text{inertia}}$. One finds that a strong torque transfers from the DED to the plasma just before the mode penetration. In other words, the rotation braking gives rise to the bifurcation of the penetration process from the suppressed to the excited state, because the amount of the magnetic reconnection depends strongly on the Doppler-shifted frequency

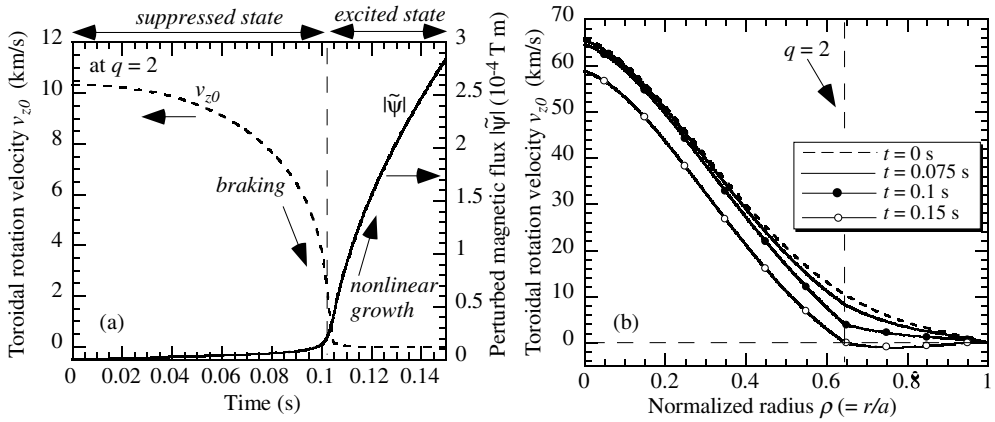

Figure 7. (*a*) Time evolutions of the toroidal rotation v_{z0} and the perturbed magnetic flux $\tilde{\psi}$ at the rational surface. Here, the $f_{\mathrm{DED}} = 0$ and the $\mu_\perp = 50\mu_{\perp 0}$. (*b*) Radial profiles of the toroidal rotation, v_{z0}.

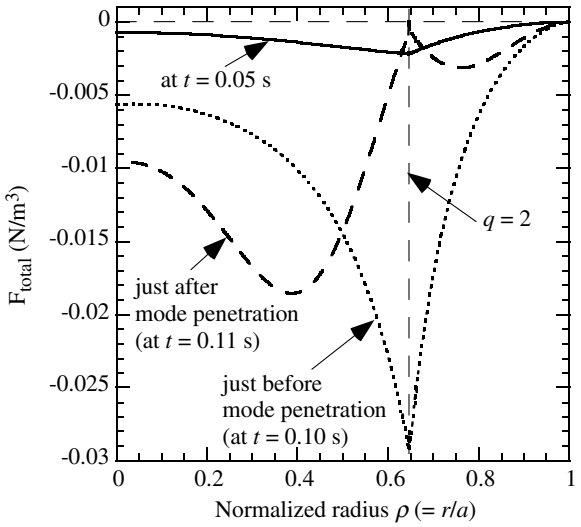

Figure 8. Radial profiles of the induced torque due to the DED. $F_{\mathrm{total}} = F_{\tilde{j}\times\tilde{B}} + F_{\mathrm{viscosity}} + F_{\mathrm{inertia}}$. The conditions correspond to figure 7.

of the DED with respect to the rotating tokamak plasma. The threshold of the required DED coil current for the mode penetration is increased (i.e. stabilizing effect) when increasing the plasma viscosity, because the viscous force ($F_{\mathrm{viscosity}}$) opposes the change in the plasma rotation due to the magnetic island. The contributions of the inertial force (F_{inertia}), which is originated from the shear flow in the vicinity of the magnetic island, are very weak in comparison with those of the viscous one. It is noticed that the perturbed magnetic flux and the toroidal rotation keep the values when the ramping of the DED coil current is stopped at a certain value during the suppressed state.

In the theory of Fitzpatrick [10] it is considered that $\tilde{j} \times \tilde{B}$ and viscous torques around the rational surface must balance in a quasi-steady state. Therefore, the bifurcation of the reconnected state could be given by the torque balance equation. On the other hand, the result

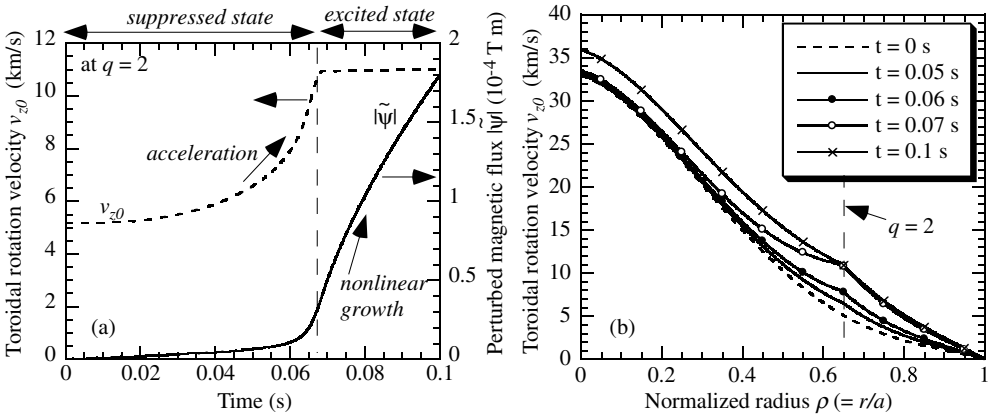

Figure 9. (*a*) Time evolutions of the toroidal rotation v_{z0} and the perturbed magnetic flux $\tilde{\psi}$ at the rational surface. Here, the $f_{\mathrm{DED}} = 1$ kHz and the $\mu_{\perp} = 50\mu_{\perp 0}$. (*b*) Radial profiles of the toroidal rotation, v_{z0}.

of the present simulation also indicates that the total induced torque, F_{total}, is zero in the vicinity of the rational surface when the bifurcation occurs. After the bifurcation the $\tilde{\psi}$ grows rapidly, and the equilibrium current density profile is flattened around the rational surface. This flattening of the current density profile is well known in nonlinear regime of tearing modes [25]. In addition, the amount of the error-field amplification is relatively small in comparison with that of the linear calculation (figure 2).

One of the interesting features of the DED is a control of the plasma rotation profile, because it is well known that a plasma rotation plays an important role for a stability of the MHD mode and an improvement of the plasma confinement [26]. Figure 9 indicates the result when the DED frequency is set to 1 kHz. The toroidal rotation, v_{z0}, is accelarated by the DED, because the induced torque acts so as to decrease the Doppler-shifted frequency between the DED and the rotating tokamak plasma. When the sign of the DED frequency is reversed, the Doppler-shifted frequency is increased, so that the required DED coil current for the mode penetration is enhanced. It is noticed again that the present model does not include effects of the plasma diamagnetic drifts.

4. Discussion

4.1. Contributions of poloidal plasma rotation

The helical magnetic perturbation induces not only a toroidal torque but also a poloidal one in the vicinity of the rational surface. Effects of the plasma poloidal rotation on the penetration process of the magnetic perturbation are the same as those of the toroidal rotation except the strong damping of the poloidal rotation due to the $\mu_{\parallel}$ [34]. Thus, it is assumed that the plasma does not respond to the poloidal torque induced by the error-field [10, 11]. However, the contribution of the poloidal rotation to the Doppler-shifted frequency between the DED and the rotating tokamak plasma cannot be neglected. Figure 10 shows time evolutions of the toroidal and poloidal rotation velocities at the rational surface, where the DED coil current is ramped linearly at $t = 0$ s. Here, the poloidal rotation, $v_{\theta 0}$, is assumed to be of the form $v_{\theta 0} = 20((r/a)^3 - (r/a)^4)$ (km s^{-1}). One finds that the threshold of the required DED coil current for the mode penetration is changed when the direction of the toroidal plasma rotation is reversed. Even though the DED is a static field, the calculated toroidal plasma rotations indicate

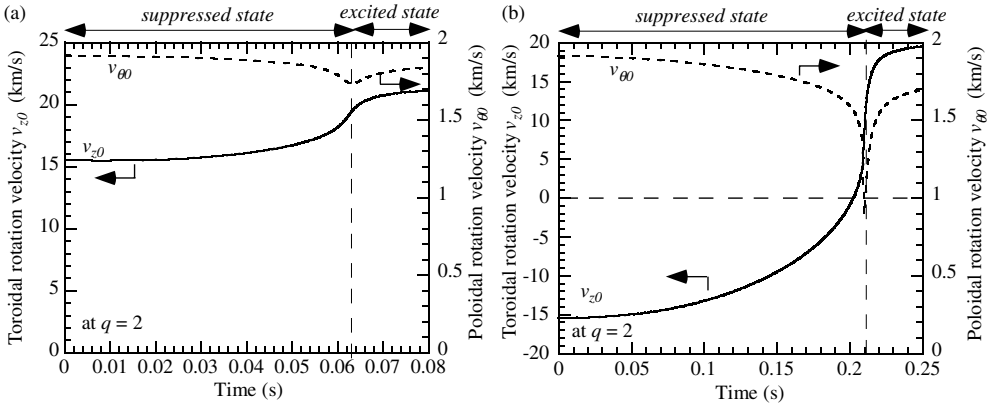

Figure 10. Time evolutions of the toroidal and poloidal plasma rotations at the rational surface. Here, $f_{\mathrm{DED}} = 0\,\mathrm{Hz}$ and $\mu_\perp = 50\mu_{\perp 0}$. The initial direction of the v_{z0} is reversed between (*a*) and (*b*).

acceleration (figure 10(*a*)) or slowing down (figure 10(*b*)). These behaviours are originated from the change of the Doppler-shifted frequency between the DED and the rotating tokamak plasma.

4.2. Comparison with experimental results on the TEXTOR

As introduced in the first section, error-field modes were onset by the DED when the amplitude of the DED coil current exceeds a certain value in the real experiments on the TEXTOR. The change of the toroidal rotation profile was observed before the mode onset (i.e. before the generation of large magnetic islands of $m/n = 2/1$) [14, 16, 17]. It seems that the change of the toroidal rotation precedes the mode onset and triggers it. This agrees well with the present model. In addition, the direction of the change of the toroidal rotation by the DED depends on the fraction of the beam power between the two tangential NBI (i.e. the sign of the toroidal rotation) and the rotation direction of the DED. Both cases (increase or slowing down) of the changes of the toroidal rotation before the mode onset can be reproduced in terms of the present model, in which the poloidal rotation is taken into account (figure 10). On the other hand, a strong neoclassical force appears due to the breakdown of the toroidal symmetry when a large locked tearing mode occurs [34]. Therefore, the change in the profile of the toroidal rotation after the mode onset cannot be reproduced by the present model. Another possible explanation, which is considered in [14, 16, 17], is that a change of the radial electric field due to the edge ergodization of the magnetic field structure gives rise to the spin-up of the toroidal plasma rotation via the momentum balance in the radial direction. Of course, the model in this study does not include this feature. However, the change of the toroidal rotation (figure 10) due to the torque transfer from the DED at the rational surface is not entirely denied. Systematic measurements of the poloidal plasma rotation could clarify the above question.

In figure 11 the required amplitude of the error-field for the mode penetration is plotted as a function of the toroidal plasma rotation velocity at the rational surface, where the poloidal rotation velocity is the same as that in figure 10. It is shown that the contribution of the small poloidal plasma rotation on the threshold of the mode penetration cannot be neglected, although the toroidal plasma rotation would be mainly changed by the tangential NBI in the real experiments. In the TEXTOR, a dependence of the threshold for the mode onset on the toroidal rotation is investigated systematically by the two tangential NBI. The latest

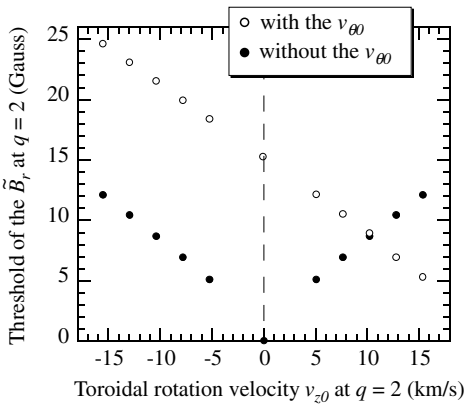

Figure 11. Dependence of the required amplitude of the error-field for the mode penetration on the plasma rotation (from the present model). The open and closed circles indicate the threshold of the required amplitude of the DED field for the mode penetration with and without the contribution of the poloidal rotation.

experimental results show that the toroidal rotation has a stabilizing effect for the mode onset, but the minimum value of the required DED coil current for the mode onset is shifted from the condition where the toroidal rotation at $q = 2$ is zero [35]. The poloidal rotation (or effects of plasma diamagnetic drifts) could affect the threshold for the mode onset as discussed in this paper (figure 11). Further experimental investigations with measurements of not only the toroidal but also the poloidal rotation could clarify this effect.

5. Summary and conclusion

In order to understand the underlying physics of the penetration process of the DED, a single fluid MHD simulation code has been developed, taking into account the plasma resistivity and the plasma viscosity. The linear model shows a localization of the induced current at the resonance surface and predicts a vortex structure of the velocity field near the resonance layer. In addition, effects of the Alfvén resonance for the error-field penetration are identified by the two peaks in the radial profiles of the perturbed toroidal current and the perturbed magnetic flux. The observed fine structures of the vorticity disappear by introducing a finite plasma viscosity. It is necessary to compare with experimental results of the error-field penetration of the DED in order to clarify the features as mentioned in this study. Direct observations of the radial profiles of the externally applied rotating magnetic perturbations with small magnetic probes inside the plasma have been performed in the small tokamak devices, CSTN-IV [36] and HYBTOK-II [37]. The present calculations show a qualitative agreement with the observed profiles in these devices.

A quasi-linear calculation shows that a sudden growth of the magnetic reconnection arises with changes of the plasma rotation. The plasma viscosity plays an important role in determining the required amplitude of the DED field for the mode penetration, because the viscous force opposes the change of the plasma rotation by the DED. It is also shown that a contribution of the small poloidal plasma rotation on the threshold of required amplitude of the DED field for the mode penetration cannot be neglected, although the toroidal plasma rotation would be mainly changed by the tangential NBI in the real experiments.

Recently, a calculation based on a linear kinetic model has been performed in order to clarify the torque transfer from the DED to the rotating plasma [38]. Effects of the plasma

diamagnetic drift, which are eliminated in the present study, are taken into account there. To extend from the present single MHD model to a two-fluid MHD model (e.g. four-field model) [39,40] is a next step of the work related to the penetration process of the DED on the TEXTOR.

Acknowledgments

One of the authors (YK) expresses his thanks for the financial support of the Japan Society for the Promotion of Science (JSPS) Postdoctoral Fellowships for Research Abroad.

References

[1] Biskamp K 2000 *Magnetic Reconnection in Plasmas* (Cambridge: Cambridge University Press) p 59
[2] Furth H P, Killeen J and Rosenbluth M N 1963 *Phys. Fluids* **6** 459
[3] Hahm T S and Kulsrud R M 1985 *Phys. Fluids* **28** 2412
[4] Wang X and Bhattacharjee A 1992 *Phys. Fluids* B **4** 1795
[5] Ma Z W, Wang X and Bhattacharjee A 1996 *Phys. Plasmas* **3** 2427
[6] Ishizawa A, Tokuda S and Wakatani M 2001 *Nucl. Fusion* **41** 1857
[7] Hender T C *et al* 1992 *Nucl. Fusion* **32** 2091
[8] Buttery R J *et al* 1999 *Nucl. Fusion* **39** 1827
[9] Buttery R J *et al* 2000 *Nucl. Fusion* **40** 807
[10] Fitzpatrick R 1998 *Phys. Plasmas* **5** 3325
[11] Lazzaro *et al* 2002 *Phys. Plasmas* **9** 3906
[12] Fitzpatrick R 2003 *Phys. Plasmas* **10** 1782
[13] Finken K H *et al* 1997 *Fusion Eng. Des.* **37** 335 Special issue devoted to the DED guest editor: Finken K H
[14] Finken K H *et al* 2004 *Plasma Phys. Control. Fusion* **46** B143
[15] Koslowski H R *et al* 2004 *31st European Conf. on Plasma Physics (London, UK, 2004)* P1-124
[16] Finken K H *et al* 2005 *Phys. Rev. Lett.* **94** 015003
[17] Wolf R C *et al* 2005 *Nucl. Fusion* **45** 1700–7
[18] Lehnen M *et al* 2005 *J. Nucl. Mater.* **337–339** 171
[19] Jakubowski M *et al* 2005 *J. Nucl. Mater.* **337–339** 176
[20] Nicolai A *et al* 2004 *Nucl. Fusion* **44** S93
[21] Strauss H R 1976 *Phys. Fluids* **19** 134
[22] Mao W and Wang M 1996 *Phys. Plasmas* **1** 946
[23] Hallatschek K 1999 *Phys. Plasmas* **6** 2495
[24] Sewell G 2005 *The Numerical Solution of Ordinary and Partial Differential Equations* 2nd edn (New York: Wiley)
[25] White R B and Monticello D A 1977 *Phys. Fluids* **20** 800
[26] Wolf R C 2003 *Plasma Phys. Control. Fusion* **45** R1
[27] Finken K H *et al* 2004 *Nucl. Fusion* **44** S55
[28] Pankratov I M *et al* 2004 *Nucl. Fusion* **44** S37
[29] Elfimov A G *et al* 2004 *Nucl. Fusion* **44** S83
[30] Lichtenberg A J *et al* 1992 *Nucl. Fusion* **32** 495
[31] Kurita G *et al* 1993 *J. Phys. Soc. Japan* **62** 524
[32] Tokar M Z *et al* 1998 *Nucl. Fusion* **38** 961
[33] Zimmermann O *et al* 2005 *32nd European Conf. on Plasma Physics (Tarragona, Spain, 2005)* P4-059
[34] Ida K 1998 *Plasma Phys. Control. Fusion* **40** 1429
[35] Koslowski H R *et al* 2005 *32nd European Conf. on Plasma Physics (Tarragona, Spain, 2005)* P4-061
[36] Kobayashi M *et al* 2000 *Phys. Plasmas* **7** 3288
[37] Kikuchi Y *et al* 2004 *Nucl. Fusion* **44** S28
[38] Heyn M *et al* 2005 *32nd European Conf. on Plasma Physics (Tarragona, Spain, 2005)* P2-020
[39] Reiser D and Scott B 2005 *32nd European Conf. on Plasma Physics (Tarragona, Spain, 2005)* P2-032
[40] Furuya A, Yagi M and Itoh S-I 2003 *J. Phys. Soc. Japan* **72** 313